A Mutant of Arabidopsis Lacking the Triose-Phosphate/Phosphate Translocator Reveals Metabolic Regulation of Starch Breakdown in the Light[1][w]

Robin G. Walters*, Douglas G. Ibrahim[2], Peter Horton, and Nicholas J. Kruger

Department of Plant Sciences, University of Oxford, Oxford OX1 3RB, United Kingdom (R.G.W., D.G.I., N.J.K.); and Robert Hill Institute, Department of Molecular Biology and Biotechnology, University of Sheffield, Sheffield S10 2TN, United Kingdom (P.H.)

The chloroplast envelope triose-phosphate/phosphate translocator (TPT) is responsible for carbohydrate export during photosynthesis. Using measurements of carbohydrates, partitioning of assimilated $^{14}CO_2$, photosynthetic gas exchange, and chlorophyll fluorescence, we show that a mutant of Arabidopsis lacking the TPT increases synthesis of starch compared to the wild type, thereby compensating for a deficiency in its ability to export triose-phosphate from the chloroplast. However, during growth under high light, the capacity for starch synthesis becomes limiting so that the chloroplastic phosphate pool is depleted, resulting in a restriction on electron transport, a reduction in the rate of photosynthesis, and slowed plant growth. Under the same conditions but not under low light, we observe release of ^{14}C label from starch, indicating that its synthesis and degradation occur simultaneously in the light. The induction of starch turnover in the mutant specifically under high light conditions leads us to conclude that it is regulated by one or more metabolic signals, which arise as a result of phosphate limitation of photosynthesis.

During photosynthesis, the triose-phosphate/phosphate translocator (TPT) of the chloroplast inner envelope membrane mediates the counterexchange of stromal triose-phosphates (triose-P) derived from CO_2 fixation with cytosolic orthophosphate (P_i), thus providing the cytosol with the precursors for Suc synthesis. Optimum rates of photosynthesis require the regulated exchange of metabolites through TPT. If triose-P is withdrawn from the chloroplast too quickly, the Calvin cycle is depleted of intermediates. Alternatively, if transport through TPT is too slow, phosphorylated intermediates accumulate in the chloroplast, resulting in a depletion of stromal P_i, which in turn has the potential to restrict ATP synthesis, again restricting CO_2 fixation (Edwards and Walker, 1983). Under normal circumstances, the potential inhibition of photosynthesis due to P_i limitation is ameliorated by activation of ADP-Glc pyrophosphorylase (AGPase; Sowokinos, 1981; Sowokinos and Preiss, 1982), leading to an increase in the rate of starch synthesis and a resulting release of P_i.

Studies on transgenic potato (*Solanum tuberosum*) and tobacco (*Nicotiana tabacum*) plants possessing altered amounts of TPT have established the central role of this translocator in the integration of assimilate partitioning during photosynthesis (Barnes et al., 1994; Heineke et al., 1994; Häusler et al., 1998, 2000a, 2000b). The patterns of carbohydrate synthesis in such plants suggest that they compensate metabolically for the reduced levels of TPT by diverting assimilate into starch, releasing the P_i required for continued photosynthesis. Remarkably, despite the changes in carbohydrate metabolism, plants with as little as 20% of wild-type TPT activity show little or no reduction in the maximum rate of CO_2 assimilation under ambient atmospheric conditions, and no change in growth rate (Riesmeier et al., 1993; Barnes et al., 1994; Heineke et al., 1994; Häusler et al., 1998, 2000a). It is proposed that Suc synthesis and export from leaves in such plants is achieved through increased starch turnover and export of carbon from the chloroplast in the form of neutral sugars, probably via the pathway used for carbohydrate export at night (Niittylä et al., 2004; Weise et al., 2004). Thus, antisense potato plants accumulate increased amounts of starch during the day that are then exported at night (Heineke et al., 1994). By contrast, antisense tobacco plants appear to maintain export of photosynthate from the leaf by amylolytic breakdown of starch in the light; in this case it was proposed that there is continuous turnover of starch in the leaves of the antisense tobacco plants throughout the day (Häusler et al., 1998, 2000a).

Recently, an Arabidopsis mutant *tpt-1* containing a T-DNA insert in the single gene encoding TPT (At5g46110) has been isolated in a reverse-genetic screen (Schneider et al., 2002). As with the antisense studies, no changes in photosynthesis or growth were reported. Severe impairment of photosynthesis and

[1] This work was supported by the United Kingdom Biotechnology and Biological Sciences Research Council (grant no. P15726).

[2] Present address: Department of Animal and Plant Sciences, University of Sheffield, Western Bank, Sheffield S10 2TN, UK.

* Corresponding author; e-mail robin.walters@plants.ox.ac.uk; fax 44 (0)1865 275074.

[w] The online version of this article contains Web-only data.

Article, publication date, and citation information can be found at www.plantphysiol.org/cgi/doi/10.1104/pp.104.040469.

growth in a *tpt-1/adg1-1* double mutant (deficient in starch synthesis) established that starch production is essential for normal growth in the absence of TPT (Schneider et al., 2002) but did not reveal the mechanism of metabolic compensation in the *tpt-1* mutant. Similarly, although it was demonstrated that the *tpt-1* mutant has a greater rate of starch mobilization in the dark (Schneider et al., 2002), the study did not establish whether starch degradation occurs in the light in parallel with photosynthesis in these plants.

To address this issue, we have examined photosynthetic carbon partitioning in the identical mutant (*ape2*), which was independently isolated in a chlorophyll fluorescence-based screen designed to identify lines defective in photosynthetic acclimation (Walters et al., 2003). Since the protocol used to identify the mutant indicated that these plants may have a defect that is specifically revealed only during growth under high light (HL), the responses of plants grown under low light (LL) and HL conditions were compared. Here, we report that although LL-grown plants exhibited altered carbohydrate partitioning, there was no effect on growth and photosynthesis was unaffected under normal growth conditions, and we could find no evidence for accelerated starch turnover in the light. By contrast, under HL growth conditions, the inability of the mutant to export triose-P normally led to reductions in both photosynthetic rate and growth rate. Furthermore, we describe $^{14}CO_2$ pulse-chase experiments, which have provided for the first time, to our knowledge, clear evidence for starch turnover in parallel with photosynthesis in the light, specifically in HL-grown *ape2* plants. We present a hypothesis in which starch turnover is triggered by a combination of reduced Suc levels in the cytosol and redox changes in the chloroplast stroma, both of which result from the restriction on photosynthesis imposed by the TPT deficiency in these plants.

RESULTS

The *ape2* Mutation Blocks Expression of the TPT

We have previously described how the *ape2* mutation is due to tandem insertion of at least two T-DNA elements immediately upstream from the *TPT* translational start site (Walters et al., 2003). This is comparable with the description of *tpt-1* (Schneider et al., 2002), which was isolated from the Feldmann T-DNA-transformed population by a reverse-genetic screen; analysis of the DNA sequence at the site of the insertion in the *tpt-1* line confirms that *tpt-1* and *ape2* carry the same T-DNA insertion (A. Schneider, personal communication). *TPT* expression is greatly reduced in the *tpt-1* line (Schneider et al., 2002). Figure 1 shows the results of an analysis of *TPT* expression in the *ape2* mutant, confirming that a similar effect is observed under our growth conditions. Analysis by quantitative reverse transcription (RT)-PCR resulted in the detection of markedly less product than for the wild type even when levels of *ape2* template were increased 10-fold (Fig. 1A), showing that *TPT* mRNA levels were less than 5% of that in the parental wild type, Ws-2; this was quantitatively in agreement with the reduction in *TPT* mRNA levels and TPT-specific transport activity in the *tpt-1* line (Schneider et al., 2002). It was also confirmed that no compensatory changes occurred in the expression of other phosphate translocators; quantitative RT-PCR provided no evidence for discernible changes in mRNA levels encoding the Glc-6-P/P translocator (GPT), phospho*enol*pyruvate/P translocator (PPT), and Xyl-5-P/P translocator (XPT) transporters (data not shown), again consistent with the data for *tpt-1* (Schneider et al., 2002).

However, postamplification restriction digestion used to distinguish individual *GPT* and *PPT* genes (Fig. 1B) showed that, while there were no changes in the relative levels of *PPT1* and *PPT2* mRNAs, clear changes could be identified in the pattern of *GPT* gene expression in *ape2* plants. These findings were confirmed in microarray experiments using leaves from the wild type and mutant grown under both LL and HL (Fig. 1C). Not only did the *ape2* mutant show no increases in mRNAs encoding phosphate translocators, but also there was a decline in *GPT2* message to below detectable levels. The significance of this change is unclear at present.

SDS-PAGE analysis of chloroplast envelope preparations confirmed that the reduced mRNA levels were reflected in decreased levels of TPT protein, and conversely that levels of other transporters were not appreciably increased. No changes in the polypeptide profile were apparent other than in a diffuse band corresponding to the TPT protein (Barnes et al., 1994), which was virtually eliminated in the mutant (Fig. 1D).

The *ape2* Mutant Has Altered Leaf Carbohydrate Content

Analysis of assimilate accumulation provided strong evidence that the decreased *TPT* mRNA levels compromised the ability of the *ape2* mutant to export triose-P from the chloroplast. Figure 2 shows the levels of hexoses, Suc, and starch extracted from the leaves of LL-grown wild-type and *ape2* plants during an 8-h photoperiod. In both lines, starch and Suc, the dominant carbohydrates, increased progressively throughout the day (Fig. 2, A and B). Levels of Glc increased but then returned to predawn levels at the end of the day (Fig. 2C). By contrast, there were no clear changes during the day in the amount of Fru in wild-type plants, although this minor component accumulated progressively in the mutant (Fig. 2D). Crucially, however, Suc levels in the leaves of the *ape2* mutant were markedly lower than those of the wild type throughout the day, despite being identical at the start of the photoperiod (Fig. 2B), while starch accumulated up to 50% faster in the mutant than in the wild type (Fig. 2A). Moreover, hexose levels were significantly lower in the mutant (Fig. 2, C and D), as would be expected if

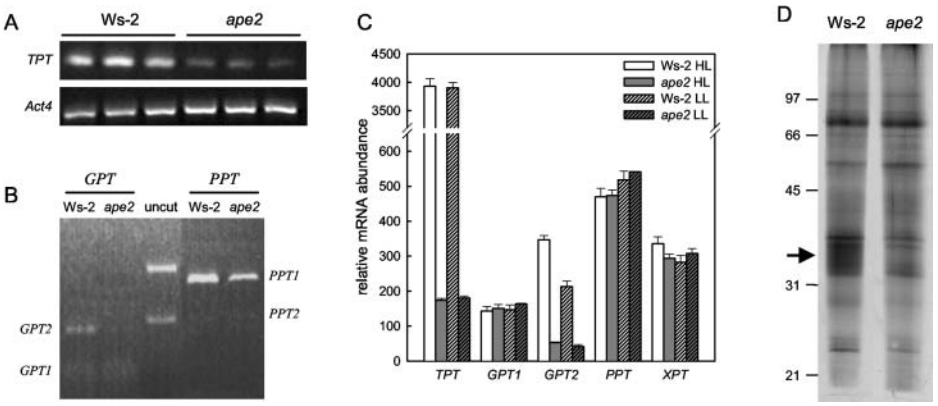

Figure 1. Expression analysis of the *ape2* mutant. Total RNA and chloroplast envelopes were isolated from leaf tissue harvested 2 h into the photoperiod. A, Quantitative RT-PCR was carried out for three independent RNA preparations as described in "Materials and Methods," with amplification of *Act4* mRNA as a loading control. The *TPT* amplification from *ape2* RNA was carried out using 10-fold more template than for the remaining reactions. B, RT-PCR amplification products for the *GPT* and *PPT* genes were purified and the relative contributions of individual genes were quantified by restriction digestion. *Xho*I gave products of 212/194 bp (*GPT1*) and 352/54 bp (*GPT2*), and *Hin*dIII plus *Pvu*II gave products of 584/93 bp (*PPT1*) and 366/308 bp (*PPT2*). Uncut amplification products from wild-type plants (*GPT*, 406 bp; *PPT*, 677 bp/674 bp) are also shown. C, Relative mRNA levels for genes encoding chloroplast envelope transporters were determined using the Affymetrix ATH1 Arabidopsis Genome Array; this microarray does not distinguish between the two *PPT* genes. Data are mean ± SE, $n = 3$. D, Protein from chloroplast envelopes (corresponding to 20 μg of leaf chlorophyll) were separated by SDS-PAGE and silver stained. The positions of molecular mass markers (sizes in kD) and the TPT protein (arrow) are as shown.

they were produced primarily as a consequence of Suc cycling.

These changes are similar to those observed previously for antisense tobacco and potato plants with reduced levels of TPT (Barnes et al., 1994; Heineke et al., 1994; Häusler et al., 1998, 2000a) and are consistent with a decrease in the rate of Suc synthesis and a change in carbon partitioning in favor of starch in the *ape2* mutant relative to Ws-2. Such changes in carbon partitioning have also been observed in mutant and antisense plants with reduced levels of cytosolic Fru-1,6-bisphosphatase, in which the pathway of Suc biosynthesis from triose-P is again disrupted (Sharkey et al., 1992; Zrenner et al., 1996; Strand et al., 2000). However, while there were qualitative similarities to the previous data for Arabidopsis *tpt-1* (Schneider et al., 2002) in terms of the effect of the mutation, there were also marked quantitative differences. In particular, our data gave rates of starch accumulation that were approximately 3-fold greater in both the wild type and mutant and of Suc accumulation that were 10-fold greater in the wild type; we also observed significant accumulation of Suc during the day in the *ape2* line, whereas there was no obvious increase in Suc throughout the photoperiod in *tpt-1*. Levels of hexoses were also consistently higher than reported previously.

To further explore the fate of recently assimilated CO_2, we carried out experiments in which intact plants were supplied with $^{14}CO_2$ during photosynthesis under normal growth conditions. Wild-type and mutant plants were labeled in the growth chamber, being placed side by side in a sealed glass tank within which $^{14}CO_2$ was released, thus ensuring that the two sets of plants were exposed to identical conditions during labeling. The quantity of supplementary $^{14}CO_2$ was sufficient to ensure that the plants did not exhaust the CO_2 within the chamber during each 15-min labeling period, but was not so high that photorespiration was completely suppressed, thereby minimizing the effects of high CO_2 levels on ^{14}C labeling patterns. The radioactivity recovered by flushing the chamber through KOH traps and extracting plant metabolites indicates that the $[CO_2]$ in the chamber was in the range 250 to 350 $\mu L\ L^{-1}$ by the end of the labeling period.

Table I shows that, under these experimental conditions, a TPT deficiency significantly altered photoassimilate partitioning under both LL and HL growth conditions. The proportion of $^{14}CO_2$ converted into Suc was lower in the *ape2* mutant than in the wild type under both LL and HL. Nevertheless, despite the TPT deficiency, the *ape2* mutant was able to export an appreciable proportion of assimilated carbon to the cytosol to make Suc. The reduced incorporation into Suc was accompanied by a parallel decrease in the proportion of ^{14}C in the minor soluble sugars Glc and Fru, while the proportion of label entering organic acids and phosphate esters was unaffected by the *ape2* mutation.

In LL, the reduced incorporation into soluble sugars was reflected in an increase in the labeling of starch, consistent with measurements of carbohydrate content (Fig. 2) and data for *tpt-1* plants labeled using saturating concentrations of $^{14}CO_2$ (Schneider et al., 2002). Thus, it appears that the mutant compensates for a TPT deficiency by diverting photoassimilate into starch. In HL, however, there was only a small (not

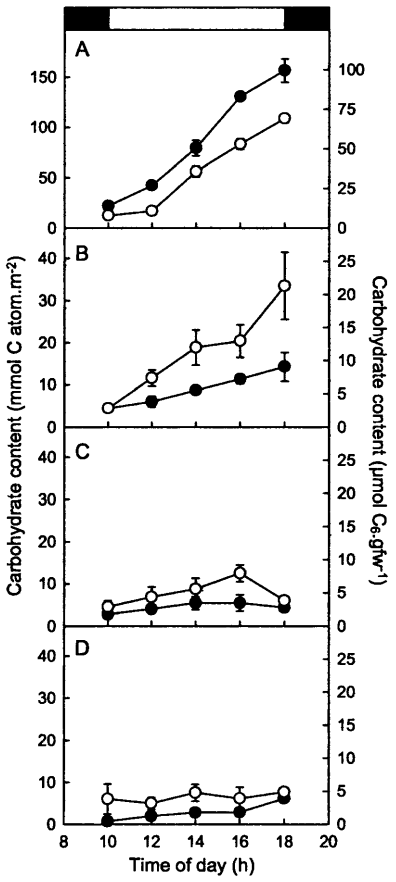

Figure 2. Altered carbohydrate accumulation in the *ape2* mutant. The carbohydrate content of leaves was determined in discs cut from LL-grown wild-type (○) and *ape2* (●) plants at 2-h intervals throughout the day. A, Starch; B, Suc; C, Glc; D, Fru. The bar at the top indicates the times of the dark-light and light-dark transitions. The data are plotted according to the left-hand axis; the right-hand axis is shown to allow comparison with previous data and corresponds to a specific leaf fresh weight of 26 mg cm^{-2}. Data are mean ± SE, $n = 4$.

statistically significant) increase in the proportion of ^{14}C in starch in *ape2* plants compared to the wild type, and there was instead a marked increase in proportional labeling of amino acids.

Changes in Carbon Flux and Starch Turnover during HL Growth

Accumulation of label in specific metabolites is influenced not only by the rate of labeling but also by the size of different metabolite pools and their rate of turnover. To further investigate how a TPT deficiency alters the fate of assimilated $^{14}CO_2$, pulse-chase experiments were carried out in which plants were harvested immediately following a period of $^{14}CO_2$ assimilation or were allowed to continue photosynthesis in the growth cabinet for a further 2 or 4 h before extraction and fractionation. Recovery of unincorporated label showed that in these experiments, there were higher overall CO_2 concentrations during the pulse, with the final [CO_2] being in the range 490 to 570 $\mu L\ L^{-1}$ (we presume the lower assimilation to be due to the lower number of plants in the chamber). Nevertheless, the initial patterns of labeling were consistent with the previous experiments, with only minor changes in the proportional labeling of amino and organic acids, which could be accounted for by reduced rates of photorespiration. Once again, the proportion of label found in Suc was lower in the mutant with a compensating increase in proportional labeling of starch not only under LL conditions but also in HL, which can again be attributed to the elevated levels of CO_2 during labeling.

By expressing the recovered counts relative to rosette size, it was possible to determine quantitatively the fate of CO_2 fixed during the pulse during normal photosynthesis in air over the following 4 h. Figure 3 shows the results of this analysis after correction for differences in the overall specific activity of the CO_2 in the chamber (to avoid depletion of CO_2 during the pulse, the quantity of $^{14}CO_2$ supplied to wild-type plants under HL conditions was larger than for the other three sets of plants). It is immediately apparent that HL wild-type plants had a markedly higher CO_2 fixation rate than the corresponding *ape2* plants (approximately 24 $\mu mol\ m^{-2}\ s^{-1}$ compared to 9 $\mu mol\ m^{-2}\ s^{-1}$), whereas the two sets of LL plants had similar CO_2 fixation rates (6 $\mu mol\ m^{-2}\ s^{-1}$). These values correspond very closely to the measured rates of CO_2-saturated oxygen evolution at the relevant actinic irradiance (Fig. 4A).

Irrespective of the initial extent of labeling during the pulse, four metabolite pools consistently showed a progressive decrease in labeling during the chase: Suc, amino acids, phosphate esters, and to a lesser extent organic acids. The rapid removal of label from these pools suggests that each is turning over rapidly, consistent with their roles as metabolic intermediates, biosynthetic precursors, and translocated substrates for metabolism in sink tissues. Conversely, labeling of protein and cell wall fractions increased during the chase, as would be expected for biosynthetic end products.

The patterns for the remaining metabolite pools were less consistent, in each case showing a somewhat different labeling pattern in the HL *ape2* plants. Glc and Fru exhibited an initial increase in label during the chase, which was consistent with these compounds being derived secondarily from the hydrolysis of Suc. In most plants there was a subsequent decrease in labeling of hexoses, particularly Fru, but in HL *ape2* plants the extent of hexose labeling was maintained. An even more dramatic difference during the chase, however, was in the labeling of starch. In LL-grown plants, labeling of starch increased, reflecting the gradual chasing of label into biosynthetic end products; this pattern was even clearer in HL-grown wild-type plants. However, HL *ape2* plants showed instead a clear decline in labeling of starch during the chase.

Table I. *Distribution of incorporated ^{14}C following assimilation of $^{14}CO_2$*

For each growth condition, six wild-type and six *ape2* plants were placed side by side in a sealed glass container in which was released 500 μL L^{-1} $^{14}CO_2$. After 15 min photosynthesis under growth light conditions, the chamber was flushed through with air and metabolism was quenched by immediately freezing leaf tissue in ethanol. The distribution of ^{14}C between metabolite fractions was determined. The data for each fraction are expressed as a percentage of total recovered label (mean ± SE, $n = 6$). The recovery of label following fractionation averaged 97%.

	HL		LL	
	Ws-2	*ape2*	Ws-2	*ape2*
Soluble	61.6 ± 1.9	59.5 ± 1.5	54.3 ± 1.0	47.9 ± 1.3[a]
Neutral sugars	32.2 ± 1.6	22.2 ± 0.8[a]	18.6 ± 0.9	10.9 ± 0.2[a]
Fructose	2.2 ± 0.2	0.8 ± 0.0[a]	0.9 ± 0.0	0.3 ± 0.0[a]
Glucose	4.6 ± 0.3	3.2 ± 0.4[b]	2.2 ± 0.1	1.2 ± 0.0[a]
Sucrose	24.9 ± 1.2	17.8 ± 0.7[a]	15.3 ± 0.8	9.1 ± 0.3[a]
Other	0.6 ± 0.1	0.5 ± 0.1	0.2 ± 0.0	0.3 ± 0.1
Amino acids	17.2 ± 2.0	23.9 ± 1.5[b]	21.6 ± 0.9	23.5 ± 0.8
Organic acids	10.5 ± 1.3	10.9 ± 0.5	12.0 ± 0.5	11.4 ± 0.6
Phosphoesters	1.6 ± 0.2	2.5 ± 0.5	2.2 ± 0.1	2.0 ± 0.2
Insoluble	38.4 ± 1.9	40.5 ± 1.5	45.7 ± 1.0	52.1 ± 1.3[a]
Starch	30.3 ± 2.1	31.9 ± 1.3	35.2 ± 1.2	41.7 ± 1.3[a]
Protein	3.1 ± 0.2	3.5 ± 0.1	4.0 ± 0.3	4.2 ± 0.2
Cell wall	5.1 ± 0.3	5.1 ± 0.3	6.5 ± 0.3	6.2 ± 0.3

[a]Significant difference from the corresponding wild type, $P < 0.005$. [b]Significant difference from the corresponding wild type, $P < 0.05$.

Photosynthesis and Growth

Figure 4 shows the results of measurements of photosynthetic gas exchange carried out on wild-type and *ape2* plants grown under LL or HL conditions. Under limiting light, the mutation had no perceptible effect on photosynthesis (Fig. 4, A and B), but as the light level was increased to the point where factors other than light become limiting, differences between the wild type and mutant became apparent, there being a significant reduction in the maximum CO_2 assimilation rate in air (350 μL L^{-1} CO_2) for both LL-grown ($P < 0.05$) and HL-grown ($P < 0.01$) plants (Fig. 4B). This difference was even more noticeable under nonphotorespiratory conditions, the *ape2* mutant having light-saturated rates of photosynthesis that were greatly reduced in comparison to the wild type (Fig. 4A).

This relative insensitivity of the *ape2* mutant to elevated CO_2 is emphasized by the A-C_i curves for HL-grown plants (Fig. 4C). Wild-type plants exhibited the anticipated rise in CO_2 assimilation rate (A) as the intercellular CO_2 concentration (C_i) increased, with an approximately linear region at low C_i (where the limiting factors were the level of activated Rubisco and the availability of CO_2 itself) and a hyperbolic region at higher C_i (where CO_2 fixation was instead dependent on the rate of regeneration of ribulose-1,5-bisphosphate, or RuBP). As would be expected, under high [CO_2] conditions, the rate of CO_2 consumption corresponded closely to the maximum rate of O_2 evolution (Fig. 4A). In contrast to the wild type, the *ape2* mutant exhibited a highly atypical A-C_i relationship—although there was the expected initial linear A-C_i response, at higher C_i (180 μL L^{-1} or above) there was no further increase in assimilation rate. Since C_i is higher than this at growth irradiance (Fig. 4D), this strongly implies that *ape2* plants suffer a limitation on RuBP regeneration, even under ambient conditions, and that this is the basis for the observed reduction in the rate of photosynthesis (Fig. 4B). The inability of HL *ape2* to increase assimilation rates in response to elevated CO_2 also accounts for the reduced amount of ^{14}C labeling during the feeding experiments compared to HL wild-type plants (Fig. 3).

Although the TPT defect restricted the maximum rate of photosynthesis in both LL- and HL-grown plants, photosynthesis under growth conditions was only affected in HL. At light levels corresponding to the plants' growth conditions, there was no difference in photosynthesis at LL, but the photosynthetic rate of HL-grown *ape2* plants was clearly lower than that of the corresponding wild-type plants (Fig. 4B). Figure 5 shows that although there was no perceptible effect of a TPT defect on growth under LL, under HL conditions the *ape2* mutation had adverse consequences for plant growth. There were decreases in rosette diameter (Fig. 5A), total leaf area, and fresh weight from early in development onward. Even in plants at similar developmental stages, the rate of rosette expansion was appreciably slower in *ape2* plants (Fig. 5B), indicating that the reduced size at any given stage of growth of *ape2* plants was not simply due to retarded seedling development. It was also notable that the onset of flowering occurred approximately a week later in the mutant, for both LL and HL growth (data not shown).

Analysis of Electron Transport

The *ape2* mutant was selected on the basis of a strong chlorophyll fluorescence phenotype (Walters et al., 2003), indicating that photosynthetic electron

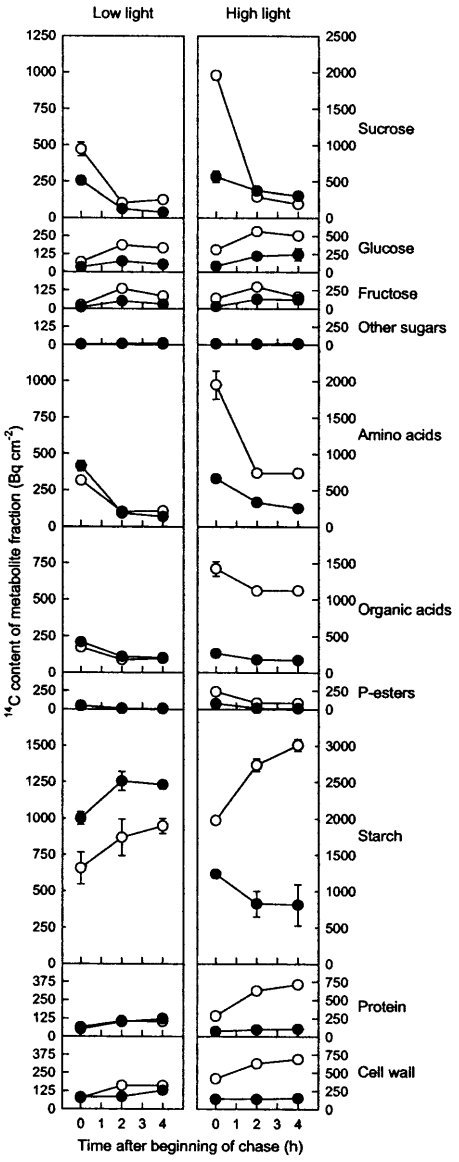

Figure 3. The fate of assimilated ^{14}C during continuing photosynthesis. Nine LL- or HL-grown wild-type (○) or *ape2* (●) plants were placed in a sealed glass container in which was released 500 μL L^{-1} $^{14}CO_2$ (1,000 μL L^{-1} for HL wild type). After 15 min photosynthesis under growth light conditions, the chamber was flushed through with air and three plants were removed either immediately or after a further 2 and 4 h, and metabolism was quenched by immediately freezing leaf tissue in ethanol. The data show the absolute ^{14}C content of metabolite fractions expressed relative to rosette area, with correction for the unlabeled CO_2 present in the chamber (mean ± SE, $n = 3$). Note the 2-fold difference between HL and LL in the scales for the *y* axes. Average recovery of label following fractionation of the ethanol-insoluble and ethanol-soluble components was 95% and 80%, respectively.

transport was perturbed—i.e. the limitation on photosynthesis in HL-grown *ape2* plants had consequences beyond carbohydrate metabolism and growth. Figure 6 shows the results of chlorophyll fluorescence measurements from wild-type and *ape2* plants in situ (i.e. under growth conditions), and chlorophyll fluorescence and PSI redox measurements carried out in parallel with the above analysis of photosynthesis (Fig. 4). Wild-type plants maintained efficient photosynthesis over a wide range of growth conditions, in situ PSII efficiency (Φ_{PSII}) falling only slightly with an increase in growth irradiance from 100 to 600 μmol quanta m^{-2} s^{-1}, consistent with our previous data for the Landsberg *erecta* accession (Bailey et al., 2004). By contrast, although photosynthetic efficiency of *ape2* plants was similar to that of the wild type under LL growth, there was a clear drop in Φ_{PSII} under HL and an even greater reduction at higher growth irradiance (Fig. 6A). Data for the fluorescence parameter 1-qP (Fig. 6B) showed that the reductions in photosynthetic efficiency arose largely as a result of changes in the redox state of the acceptor side of PSII, reflecting a more reduced plastoquinone pool. There was no significant difference in the redox state of PSII during growth of wild-type plants under a wide irradiance range, and although *ape2* plants maintained a similar PSII redox state during LL growth, growth under HL resulted in a clear increase in the proportion of PSII (and plastoquinone) in the reduced state in the mutant. This effect was even more pronounced under yet higher growth light.

To complement these data, measurements of chlorophyll fluorescence and PSI redox state (via measurements of 830-nm absorption changes) were made in parallel with the photosynthesis measurements (Fig. 4). Under these conditions, a difference in PSII redox

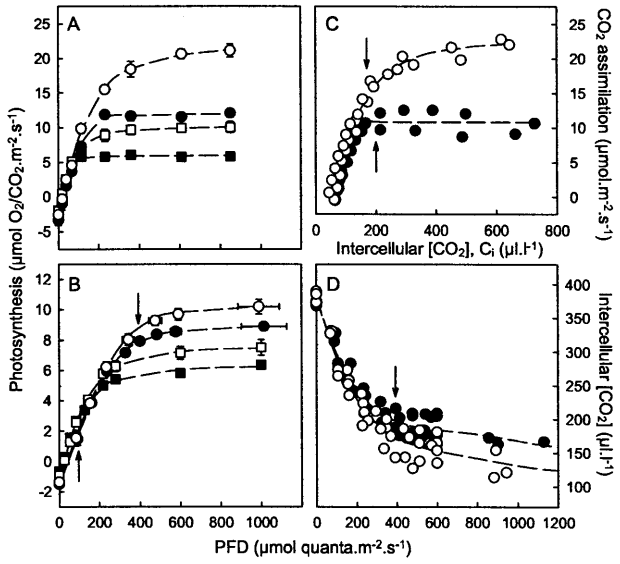

Figure 4. Decreased photosynthetic rates in the *ape2* mutant. Light response curves for O_2 evolution in saturating CO_2 from leaf discs (A) and CO_2 consumption by attached leaves in ambient (350 μmol mol^{-1}) CO_2 (B), for wild-type (○,□) and *ape2* (●,■) plants grown under HL (○,●) or LL (□,■). Arrows in B indicate the light levels corresponding to LL and HL growth conditions. C, Dependence of light-saturated CO_2 consumption on intercellular [CO_2] for HL-grown plants. Arrows indicate the values for C_i corresponding to ambient external [CO_2] at HL light levels, as determined from the light response curves for intercellular [CO_2] for HL-grown plants (D).

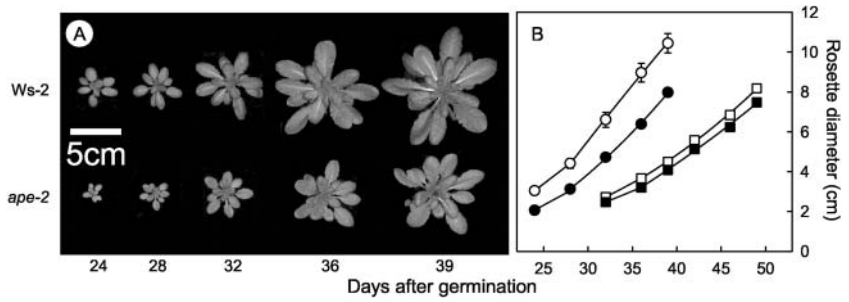

Figure 5. Slower growth in the *ape2* mutant. A, Images showing the growth of representative wild-type and *ape2* plants under HL conditions. B, Rosette diameter determined from images of wild-type (○,□) and *ape2* (●,■) plants, grown side by side under HL (○,●) or LL (□,■). Data are mean ± SE, $n \geq 6$.

state was again observed in HL-grown plants at light levels corresponding to growth conditions (Fig. 6C), which was accompanied by a change in the PSI primary electron donor (P700) to a more oxidized state in *ape2* plants than in the wild type (Fig. 6E). No PSI redox changes were observed for LL-grown *ape2* plants (data not shown).

Taken together, the redox changes on the PSII acceptor side and the PSI donor side represent a marked increase in the intersystem electron gradient in the mutant, despite the reduction in the rate of linear electron transport whether measured via CO_2 assimilation (Fig. 4B) or calculated from data for Φ_{PSII} (data not shown). This indicates a restriction on electron flow through the cytochrome b_6/f complex, which appears to have resulted from an increase in the trans-thylakoid ΔpH (Kramer et al., 1999): HL *ape2* plants exhibited an increase in chlorophyll fluorescence nonphotochemical quenching at growth irradiance (Fig. 6D), indicating that under these conditions the ΔpH was larger in the mutant (Krause and Weis, 1991), and there was a dramatic change in HL *ape2* plants in the de-epoxidation state (DES) of the xanthophyll cycle carotenoids leaves harvested directly from the growth cabinet (Table II), again indicative of an elevated ΔpH (Eskling et al., 1997). There were also parallel oscillations in the redox states of PSI and PSII in the *ape2* mutant following transient changes in light level (Fig. 6G), suggesting perturbed regulation of electron transport consistent with an increased ΔpH. Such oscillatory behavior is commonly observed when photosynthesis is limited by phosphate availability (Walker, 1992).

To assess stromal redox state in situ, the activation state of chloroplast NADP-dependent malate dehydrogenase (NADP-MDH) was determined in extracts of leaves frozen immediately after removal from growth conditions. Table II shows these data, demonstrating that the activation state of NADP-MDH was identical for wild-type and *ape2* plants under LL growth and also for HL-grown wild-type plants, but that a significant increase in NADP-MDH activation was observed in HL-grown *ape2* plants. Since NADP-MDH activation depends on electron donation from

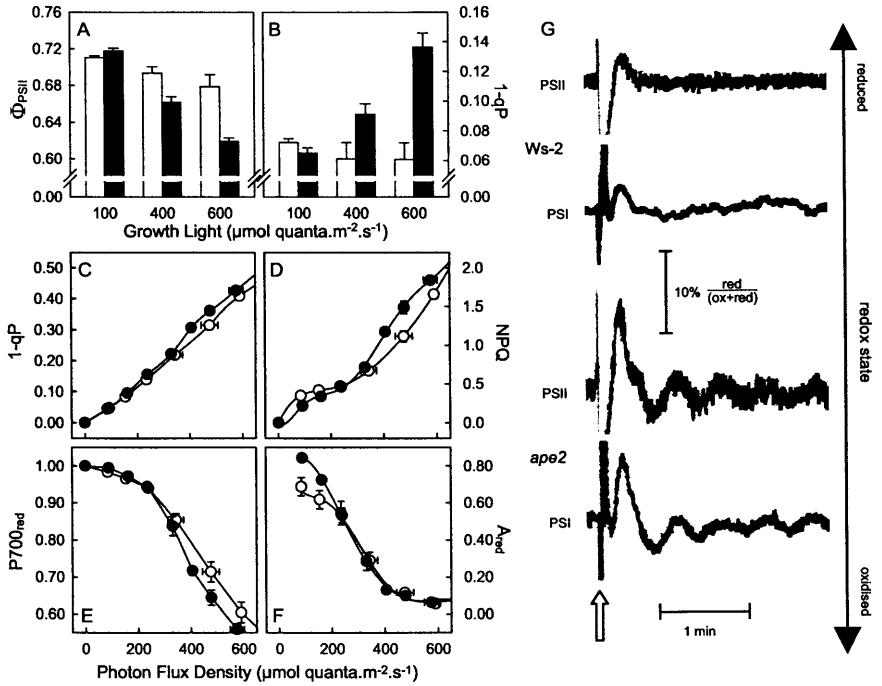

Figure 6. Chloroplast redox changes in the *ape2* mutant. A, Photosynthetic efficiency (Φ_{PSII}) and (B) PSII redox state (1-qP) determined in situ under three different growth irradiances for wild-type (white bars) and *ape2* (black bars) plants. C, 1-qP; D, nonphotochemical quenching (NPQ) of chlorophyll fluorescence; E, $P700_{red}$, the proportion of the primary donor of PSI in the reduced state; and F, A_{red}, the proportion of the primary acceptor of PSI in the reduced state, each measured in parallel with photosynthesis (see Fig. 4B) for HL-grown wild-type (○) and *ape2* (●) plants. All data are mean ± SE, $n \geq 4$. G, Oscillations in the redox states of PSII and PSI in leaves from HL-grown plants, during illumination at light levels corresponding to HL growth conditions. The figure shows traces for chlorophyll fluorescence (PSII) and A_{830} (PSI) induced by a 1-s pulse of intense light followed by 1 s darkness (arrowed). The scale bar indicates the extent of the observed redox changes in PSI and PSII.

Table II. *Carotenoid composition and NADP-MDH activation state*

Leaves were taken from plants under growth conditions 2 h into the photoperiod and were immediately frozen. They were subsequently used either for pigment extraction and analysis by reverse-phase HPLC or in assays of NADP-MDH activation state. For comparison, the NADP-MDH activation states of LL and HL wild-type plants transferred to saturating light levels for 30 min were 75 ± 1 and 69 ± 3 respectively, while in leaves darkened for 30 min it was 0.3 ± 4.3. All data are mean ± SE, $n = 4$ to 5.

	HL		LL	
	Ws-2	*ape2*	Ws-2	*ape2*
Percentage total carotenoids				
Lutein	44.3 ± 0.9	41.7 ± 0.5	46.1 ± 0.1	48.4 ± 1.3
β-Carotene	27.3 ± 1.6	28.5 ± 0.7	30.0 ± 0.5	24.1 ± 2.5
Neoxanthin	7.6 ± 0.3	7.8 ± 0.3	9.2 ± 0.2	10.9 ± 0.5
Violaxanthin	14.9 ± 0.8	9.9 ± 0.7	14.1 ± 0.5	15.6 ± 1.3
Antheraxanthin	4.4 ± 0.2	5.9 ± 0.4	0.6 ± 0.0	1.0 ± 0.4
Zeaxanthin	1.5 ± 0.2	6.1 ± 0.9	0.0 ± 0.0	0.0 ± 0.0
Xanthophyll DES (%)	17.8 ± 1.8	41.0 ± 3.2	2.1 ± 0.1	3.0 ± 1.2
NADP-MDH activation state (%)	53.5 ± 1.7	70.0 ± 1.8	53.3 ± 1.7	56.6 ± 1.9

thioredoxins and on a high NADPH to $NADP^+$ ratio (Scheibe and Stitt, 1988; Ashton et al., 2000), we conclude that the stroma of HL-grown *ape2* plants is more reduced that that of the corresponding wild type. However, this was not reflected in the redox state of the PSI primary acceptor A, for which no redox differences were identified at growth light levels, even though there were changes under low irradiance (Fig. 6D). Once again, no changes were observed in LL-grown plants (data not shown). Thus, the restriction on electron flow through the b_6/f complex prevents overreduction of PSI and the resulting generation of reactive oxygen species (Ott et al., 1999).

Analysis of the Starch Metabolism Transcriptome

It has previously been reported in transgenic lines with reduced TPT that there are changes in the activities of enzymes involved in both the synthesis and breakdown of starch (Heineke et al., 1994; Häusler et al., 1998, 2000a). In view of the possibility that redox or sugar-sensing signals could affect expression of the genes encoding such enzymes, our microarray data were analyzed for evidence of such transcriptional regulation. Figure 7 shows that only minor differences were observed between plants grown under HL and LL and that although the mRNA abundances of a few genes involved in starch metabolism were increased in *ape2* compared to the wild type, these changes were invariably small. The sole exception was *At5g18670*, whose transcript was absent from wild-type leaves but present in appreciable amounts in the *ape2* mutant; this gene encodes a putative β-amylase, which lacks an identifiable N-terminal leader peptide and which is therefore likely to be located in the cytosol. However, perhaps contrary to expectations, the clearest

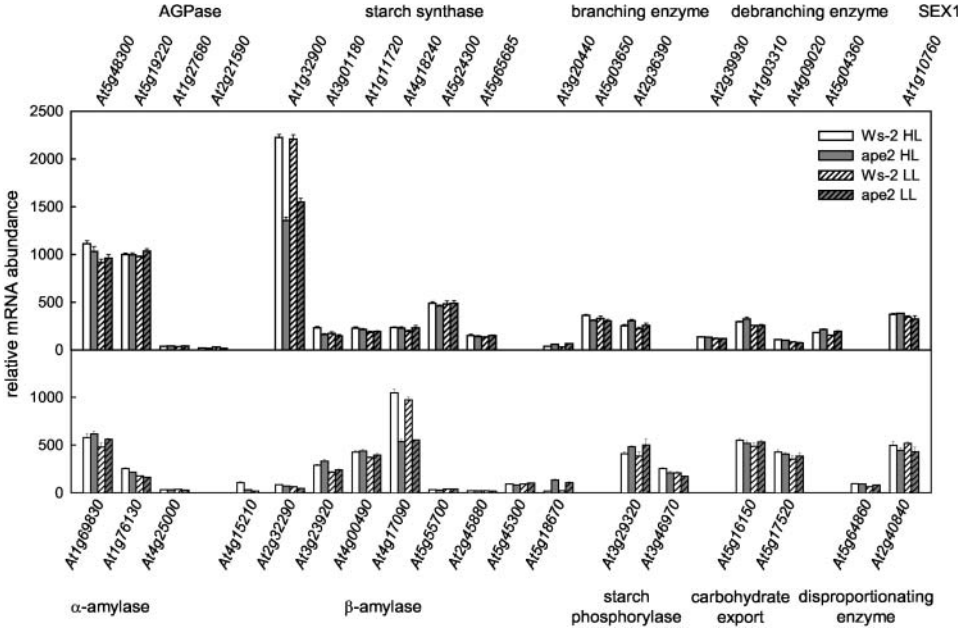

Figure 7. Expression analysis of starch metabolism genes. Total RNA was isolated from leaf tissue harvested 2 h into the photoperiod, and relative mRNA levels were determined using the Affymetrix ATH1 Arabidopsis Genome Array. The data shown are for genes known or predicted to encode proteins involved in starch synthesis, granule organization, starch breakdown, and export and utilization of starch breakdown products. Transcripts for all genes except *At3g20440* were present at detectable levels for at least one treatment. Data are mean ± SE, $n = 3$. The data on which this figure is based are available as supplemental material at www.plantphysiol.org.

consequences of a TPT deficiency were marked reductions in the mRNA levels for *At1g32900* encoding a granule-bound starch synthase and for *At4g17090* encoding a chloroplast β-amylase; it is notable that, in terms of hybridization signal, these two genes represent the most abundant of all genes involved in starch synthesis and degradation, respectively. Thus, the increased rates of starch synthesis and breakdown (whether in light or dark) in *ape2* plants are not readily explained in terms of altered gene expression.

DISCUSSION

Since the *ape2* line used in this study (Walters et al., 2003) and the *tpt-1* mutant (Schneider et al., 2002) have identical DNA sequences at the sites of the T-DNA insertions (A. Schneider, personal communication), it is clear that these independently isolated lines carry the same mutation. In both cases, the T-DNA insertion leads to a reduction in *TPT* mRNA abundance to <5% of wild-type levels, and TPT activity and protein levels are dramatically reduced (Fig. 1; Schneider et al., 2002). Thus, although it is clear from both RT-PCR and microarray analyses that the mutant retains discernible expression of the *TPT* gene, so that this does not represent a true knockout line, the residual levels of TPT activity are very small—much lower than in any previous transgenic or mutant plant. Therefore, these two Arabidopsis lines provide a powerful tool for investigating the partitioning of photosynthate. The initial characterization of the *tpt-1* mutant (Schneider et al., 2002) confirmed the influence of TPT activity on the relative proportions of fixed carbon, which are directed toward starch and Suc, and emphasized the importance of starch synthesis as a compensating metabolic pathway enabling the maintenance of high rates of photosynthesis, as shown previously in transgenic potato (Hattenbach et al., 1997). We have extended this analysis, providing direct evidence that a TPT deficiency can lead to starch turnover in the light.

Although in this study the levels and rates of accumulation of carbohydrates in the *ape2* line are greater than those reported previously for *tpt-1* (Schneider et al., 2002), there are also differences in the data for wild-type plants in the two studies. This suggests an experimental basis for the discrepancies, which are most likely the result of the different growth conditions used in the two studies. It is particularly noticeable that our plants had maximum photosynthetic rates (Fig. 4), which were also severalfold greater than those reported by Schneider et al. (2002), and thus many of the differences between the two sets of data can be ascribed to the greater supply of photosynthate in our plants. In addition, in our experiments plants were grown under an 8-h photoperiod and had largely exhausted their starch reserves by the end of the night, so that both starch and Suc levels began from a low level at the start of the day and increased as the day progressed. By contrast, the previous studies on the *tpt-1* mutant found that plants grown under a 12-h photoperiod retained appreciable starch at the end of the night, indicating that starch reserves were sufficient to sustain Suc synthesis throughout the night so that Suc levels did not vary greatly. It is notable that daylength also had clear effects on the time of flowering—we observed a marked retardation of flowering in the *ape2* line, whereas a marginal acceleration was reported for *tpt-1* (Schneider et al., 2002) and was also observed for *ape2* under long days (data not shown).

Perhaps the clearest consequence of a TPT defect is a marked reduction (approximately 50%) in the light- and CO_2-saturated rate of photosynthesis, as was the case for potato and tobacco as well as Arabidopsis *tpt-1* plants (Hattenbach et al., 1997; Häusler et al., 2000a; Schneider et al., 2002). Measurements of the C_i dependency of CO_2 assimilation showed that this was not a result of reduced carboxylation capacity but was instead due to a limitation on the regeneration of RuBP, implying a reduced availability of ATP and/or NADPH. These data also made clear that the reduction in maximum rates of photosynthesis were attributable to the inability of *ape2* plants to respond to increases in C_i above 200 μL L^{-1} (i.e. suppression of photorespiration did not result in greater availability of ATP and NADPH for CO_2 fixation). This oxygen insensitivity (so-termed because of the similar suppression of photosynthesis when O_2 partial pressure is reduced) most frequently occurs when there is a limitation on triose-P utilization (e.g. where there is reduced starch or Suc synthesis) so that P_i is sequestered, leading to low stromal P_i and a restriction on ATP synthesis (Sharkey et al., 1986)—such as is expected to occur in a TPT-deficient mutant. It is notable that a similar A-C_i relationship is observed in cytosolic Fru-1,6-bisphosphatase antisense lines (Strand et al., 2000).

Several other aspects of *ape2* behavior under light-saturating conditions were consistent with a phosphate limitation arising from accumulation of triose-P. First, an increase in the trans-thylakoid ΔpH was implied by the clear increase in ΔpH-dependent photoprotective processes within the PSII light-harvesting system and an associated change in xanthophyll DES. Second, the increased electron gradient across the cytochrome b_6/f complex indicates a restriction on plastoquinol oxidation, also indicative of a more acidic lumen and therefore an increased ΔpH (Kramer et al., 1999). Third, transient changes in light level induced sustained, parallel oscillations in the redox states of PSI and PSII. Such oscillatory behavior is consistent with a perturbation in the regulation of electron transport and has been observed previously under conditions where phosphate is limiting for photosynthesis (Walker, 1992). An increased ΔpH directly implies the presence of a constraint on its dissipation via ATP synthesis; that this arises from a phosphate limitation rather than a reduction in ATP utilization is evidenced by the activation state of NADP-MDH under growth

conditions, from which it is clear that there is normal or increased NADPH availability (Scheibe and Stitt, 1988; Ashton et al., 2000).

The reduction in maximum photosynthetic rate was not limited to CO_2-saturated conditions. Even at ambient CO_2 concentrations, there were clear reductions in photosynthetic capacity as a result of the *ape2* mutation. This is a further contrast with the findings of Schneider et al. (2002), which we again ascribe to the differences in growth conditions. *ape2* plants grown under our LL growth conditions had a dramatically (>2-fold) greater photosynthetic capacity than was reported for *tpt-1* plants grown at similar light levels, and we suggest that the effect of the TPT deficiency is only observed under conditions where other factors are not limiting growth and/or photosynthesis—indeed, we have observed that the obvious growth phenotype of HL-grown *ape2* plants was less apparent when plants were grown on a different compost (data not shown). It is clear from examination of the C_i-dependency data that the decreased photosynthetic capacity under these conditions was also a consequence of the phosphate limitation, but with the effect being less obvious due to the lower rates of photosynthesis in wild-type plants. Crucially, the restriction on photosynthesis occurred at values of C_i comparable to those observed for HL light levels, indicating that a phosphate limitation applied under HL growth conditions. Indeed, no other explanation is readily apparent for the decreases observed for HL *ape2* plants in photosynthesis (approximately 10%; Fig. 4B), in situ photochemical efficiency of PSII (approximately 10%; Fig. 6A), and the rate of rosette expansion (approximately 20%; Fig. 5). By contrast, rates of in situ photosynthesis in LL plants are low enough that they are not affected by a decreased maximum rate in *ape2* plants, so that none of these effects were observed for growth in LL, in agreement with the data for *tpt-1* (Schneider et al., 2002).

ape2 Plants Successfully Compensate for a TPT Deficiency during LL Growth

LL-grown *ape2* plants displayed a marked increase in partitioning of photosynthate into starch at the expense of Suc, as shown from carbohydrate measurements during the day and by determination of the fate of ^{14}C following a short exposure to $^{14}CO_2$ (Table I; Figs. 2–3). The labeling patterns during the following chase indicated that there were no changes in carbohydrate metabolism other than those arising as a direct result of the altered partitioning (Fig. 3). Thus, initial labeling of Suc, amino acids, organic acids, and phosphate esters was followed by progressive decreases in ^{14}C content during the chase, consistent with their roles as metabolic intermediates, biosynthetic precursors, and translocated substrates for metabolism in sink tissues; in parallel with this, there was an increase in labeling of Glc and Fru from a low initial level, consistent with these compounds being derived secondarily by hydrolysis of Suc, and there was an increase in label found in starch, protein, and cell wall components during the chase, reflecting their status as metabolic end products.

These data for LL-grown *ape2* plants are consistent with the previous findings for antisense lines of potato and tobacco as well as the *tpt-1* line (Barnes et al., 1994; Heineke et al., 1994; Häusler et al., 1998; Schneider et al., 2002), with increased starch synthesis compensating for reduced rates of Suc synthesis, thereby ensuring continued release of the phosphate needed for ATP synthesis and CO_2 fixation. This additional starch is largely absent by the end of the night (Fig. 2), indicating that there is an increased rate of starch breakdown in the dark as shown by Schneider et al. (2002). Such starch breakdown can provide the substrates needed during the night for metabolism and for Suc export to the rest of the plant (Fig. 2), as is the case in TPT antisense potato plants (Heineke et al., 1994). Thus, although carbohydrate partitioning is altered in the mutant, the overall supply of carbohydrate is unchanged (since photosynthesis in situ proceeds at the same rate), presumably explaining the unchanged growth rate of the *ape2* mutant in LL growth conditions (Fig. 5).

Despite the TPT deficiency in *ape2* plants, they nevertheless accumulated Suc during the day (Fig. 2) and incorporated ^{14}C label into Suc during the pulse (Table I; Fig. 3), in each case at approximately 50% of the rate observed in the wild type. It has been suggested that this Suc derives from simultaneous starch synthesis and breakdown in the light with subsequent export from the chloroplast, probably via the usual pathway for night-time carbohydrate export (Schneider et al., 2002); the previous work using antisense tobacco or the *tpt-1* Arabidopsis line found that TPT-deficient lines had accelerated starch turnover (Häusler et al., 1998, 2000a; Schneider et al., 2002). However, the key experiments demonstrating turnover of recently synthesized starch focused exclusively on starch breakdown during incubation of leaf discs or detached leaves in the dark. By contrast, our pulse-chase experiments were carried out using intact plants under growth conditions, so that changes in the pattern of labeling during the chase directly reflected photosynthetic metabolism. Using this approach, we found no evidence for starch turnover in the light in LL-grown *ape2* plants. Indeed, as metabolic intermediates turned over during the chase, there was an increase in ^{14}C labeling of starch quantitatively similar to that observed in the wild type. Furthermore, label was rapidly removed from Suc during the chase and was not replaced by label derived from starch turnover (in contrast to the situation for HL-grown *ape2*; see below).

Thus, although we cannot rule out a low rate of starch turnover, any such turnover cannot be sufficient to explain the observed rate of Suc synthesis. It therefore seems inevitable that the observed rate of Suc synthesis is supported by residual TPT present in the mutant and/or by other transporters with low

abundance (e.g. GPT, XPT) or with low affinity for triose-P (PPT). The higher triose-P and 3-phosphoglycerate (3PGA) levels in the chloroplast (Schneider et al., 2002) may well serve to drive transport through any of these translocators at higher rates than under normal physiological conditions in the wild type. It was previously found that, even after taking account of compensatory mechanisms, Suc synthesis was maintained at high levels (65% of wild type) in antisense tobacco plants with large decreases in TPT levels (to 30% of wild type; Häusler et al., 2000b), indicating that low levels of TPT are still able to support large rates of Suc synthesis. Synthesis of even a fraction of Suc by the normal pathway, via export of carbohydrate from the chloroplast as triose-P, would provide a trivial explanation for the largely unaltered pattern of Fru-2,6-bisphosphate levels observed in the *tpt-1* line (Schneider et al., 2002). Thus, it would appear that to term this line a knockout is perhaps inaccurate.

Simultaneous Starch Synthesis and Breakdown during HL Growth

In the initial feeding experiments where CO_2 levels were comparable to atmospheric conditions, HL-grown *ape2* plants had lower overall rates of photosynthesis, and the proportion of ^{14}C incorporated into starch was unchanged compared to the wild type (Table I). Thus, in contrast to the situation under LL, there was no increase in the net incorporation of ^{14}C into starch in the HL *ape2* plants compared to the wild type. However, it is important to consider the possibility that a significant proportion of starch synthesis may be masked by appreciable turnover, affecting the net accumulation of labeled starch. Based on relative rates of photosynthesis (Fig. 4) and the proportions of label found associated with Suc (Table I), we estimate that the rate of Suc synthesis in HL *ape2* plants was 6-fold greater than in LL *ape2* plants. Since triose-P export is presumably already approaching saturation in LL *ape2*, we conclude that some or all of the additional labeling of Suc in HL *ape2* results from starch turnover (see below).

Further information about the rate of starch synthesis in HL *ape2* plants comes from the pulse-chase experiments, in which label was determined relative to leaf area to give a measure of absolute rates of synthesis. Immediately following the pulse, there was a marked decrease in starch labeling in the mutant compared to the wild type, which could barely be accounted for by starch turnover as reflected in the rate of Suc labeling (see above). Thus, we again found no evidence for appreciable stimulation of starch synthesis relative to the wild type.

Apart from triose-P export via the TPT, starch synthesis is the dominant pathway by which a chloroplast's supply of inorganic phosphate can be readily replenished. Its importance in this regard has been shown using both Arabidopsis *tpt-1/adg1* double mutants and antisense potato plants with reduced TPT and AGPase levels (Hattenbach et al., 1997). The reduced rates of triose-P exchange/utilization resulting from such deficiencies in both TPT and AGPase have adverse consequences for photosynthesis and growth similar to those observed in HL-grown *ape2*. In view of the failure of HL *ape2* plants to stimulate starch synthesis, we conclude that the phosphate limitation experienced by *ape2* plants under HL arises because they have insufficient capacity for starch synthesis to maintain the required rate of triose-P utilization, so that phosphate is sequestered as triose-P accumulates.

The precise nature of such a limitation in HL *ape2* plants cannot be unambiguously determined from our data. The rate of starch synthesis failed to increase despite a presumed increase in the availability of hexose phosphates and an increase in the stromal ratio of 3PGA to P_i (Schneider et al., 2002), both of which should stimulate starch synthesis through activation of AGPase (Sowokinos, 1981; Sowokinos and Preiss, 1982; Hendriks et al., 2003). It is unlikely that there is a reduction in levels of AGPase protein, since there is no change in the mRNA abundance for the genes encoding AGPase (Fig. 7). One possibility might be that stimulation of AGPase activity by a high 3PGA to P_i ratio is counteracted by the decreased Suc levels in *ape2* plants (Fig. 2)—Suc has been shown to influence the covalent regulation of AGPase activity, affecting its sensitivity to elevated 3PGA and lowered phosphate levels in Arabidopsis leaves (Hendriks et al., 2003) and potato tubers (Tiessen et al., 2002; Tiessen et al., 2003). However, any effect of low Suc on AGPase activity does not affect the ability of LL-grown *ape2* plants to compensate for reduced triose-P export through a shift in partitioning of photoassimilate into starch. An alternative possibility is that the capacity for starch synthesis in HL *ape2* plants is limited due to reduced levels of the major granule-bound starch synthase encoded by the *At1g32900* gene (Fig. 7). Such a reduction would be unlikely to affect LL-grown plants in which the rate of starch synthesis is lower.

Although during the pulse-chase experiments wild-type plants assimilated markedly more $^{14}CO_2$ under HL than did *ape2* mutants (Fig. 3), as a direct result of its higher rate of CO_2 assimilation under the CO_2-enriched conditions used for $^{14}CO_2$ feeding (Fig. 4A), the subsequent 4-h chase was carried out at atmospheric CO_2 concentrations. The subsequent labeling patterns during the chase can therefore be taken to accurately reflect the pattern of carbon metabolism in ambient conditions. Indeed, the overall labeling pattern in HL wild type was qualitatively similar to that observed for both sets of LL plants, the only minor exception being the slow release of label from the organic acid pool (also observed in HL *ape2* plants), which perhaps reflects a larger organic acid pool size in HL-grown plants. Once the difference in the initial extent of labeling is accounted for, other marked differences between wild type and mutant are made clear, several of which are distinct from those seen during LL growth. Most significant was the clear

reduction in ^{14}C label found in starch in the *ape2* mutant, which occurred during the chase. Whereas wild-type plants accumulated further label, the additional ^{14}C being derived from that initially incorporated into Suc and amino acids (and also organic acids and phosphate esters), *ape2* plants showed a 30% decline in starch labeling within 2 h (Fig. 3), providing for the first time, to our knowledge, direct evidence that in TPT-deficient plants, newly synthesized starch may be broken down at the same time as ongoing starch synthesis.

Further evidence for starch breakdown in the light and an indication of the likely fate of the released label comes from the ^{14}C-labeling pattern of Suc (Fig. 3). In LL plants and HL-grown wild type, significant initial labeling of Suc was dramatically reduced 2 h later by 75% to 85%, probably reflecting Suc export to nonaerial tissues and/or reintroduction into metabolism via hydrolysis to Glc and Fru followed by phosphorylation by hexokinases; meanwhile, labeling of hexoses peaked after 2-h chase and then declined in the following 2 h, consistent with hexoses being derived from Suc breakdown and then re-entering metabolism after phosphorylation by hexokinases. However, HL *ape2* plants maintained labeling of Suc over a much longer time period—after 2 h, ^{14}C in Suc was still over 65% of the initial level (50% after 4 h)—and labeling of hexoses was also extended over a longer period with no chasing out of label after 4 h. Thus, the continued availability of labeled Suc in turn contributed to sustained levels of labeled hexoses, adding to those produced during export of label from chloroplasts following starch breakdown.

Both observations reinforce the hypothesis that there is breakdown of newly synthesized starch in the light, providing a continued supply of labeled substrates for Suc synthesis. Estimates of the rates of such breakdown indicate that this is not a minor pathway but accounts for a significant proportion of fixed carbon. Even when making the most conservative assumptions, for instance ignoring turnover of unlabeled starch synthesized before or after the pulse of $^{14}CO_2$, we calculate that the minimum rate of starch breakdown in the light is one-quarter of that which occurs at night. More realistic assumptions suggest that the rates of breakdown in the light and at night are comparable. A simple illustration of this is that, assuming our labeling experiment reflects the behavior of starch synthesized throughout the day (see Schneider et al., 2002), about one-third of starch synthesized is subsequently released during the 8-h light period, leaving the remaining two-thirds to be degraded during the subsequent 16-h dark period.

Although we cannot formally exclude the possibility that the turnover of insoluble glucan observed in this study represents the metabolism of soluble preamylopectin or phytoglycogen-like precursors prior to incorporation into starch granules, this seems unlikely. Recent pulse-labeling studies of starch indicate that after 10 min the size distribution of labeled glucan chains matches that of the glucan chains of amylopectin within the native starch granule, and it has been estimated that during the day it takes about 1 min to form each 9-nm lamella of a starch granule (Nielsen et al., 2002). Thus, the vast majority of radioactivity incorporated into starch molecules following 15 min photosynthesis in $^{14}CO_2$ is likely to be associated with granules. Given the magnitude of the loss of radioactivity from starch during the subsequent chase period in the light (Fig. 3), we believe that much of the release of label from insoluble glucan must result from turnover of starch associated with insoluble granules.

It is probable that the processes involved in the observed starch turnover during the day are the same as those responsible for starch breakdown at night. In microarray experiments using RNA from leaves taken at mid-morning (i.e. the same time of day as the $^{14}CO_2$-feeding experiments), genes involved in starch degradation and subsequent carbohydrate export exhibited no changes in the mRNA levels that correlated with the occurrence of starch turnover (Fig. 7). Although we cannot exclude the possibility that there are changes in mRNA abundance at other times of day—some genes have diurnal patterns of expression with transcription occurring principally during the latter part of the day—such changes are unlikely to be relevant to the observed mid-morning turnover of ^{14}C starch. Thus, there is no evidence for the expression of additional pathways for starch degradation in this study.

Regulation of Starch Turnover by Intrachloroplastic Signals

Our analysis of the starch metabolism transcriptome shows that the same changes are seen in *ape2* plants whether grown under HL or LL (Fig. 7). The observed changes in gene expression are intriguing in that, despite an increased requirement for starch synthesis in *ape2* plants, there is a decrease in levels of mRNAs whose protein products are required for starch synthesis and degradation. This is likely to be a response brought about by the reduced levels of Suc and hexoses in the mutant (Fig. 2). Wild-type plant would normally respond to such decreased sugar levels by altering partitioning of photosynthate away from starch and toward Suc. However, since reduced levels of starch synthase have no impact on starch synthesis in LL *ape2* plants, it seems unlikely that the transcriptional regulation highlighted by the mutant in Figure 7 plays a direct role in controlling carbohydrate partitioning in wild-type plants. It is more likely that regulation of partitioning in response to low sugar levels occurs by well-established posttranscriptional mechanisms, including allosteric and covalent regulation of AGPase. In this context, the apparent limitation on starch synthesis in HL *ape2* plants appears to be an inadvertent consequence of an increased requirement for starch synthesis in the presence of a signal indicating a supposedly reduced requirement.

The induction of starch turnover in HL *ape2* plants is not simply a result of changes in mRNA abundance, since the same pattern of gene expression is observed in LL *ape2* plants, which do not exhibit starch turnover in the light. Furthermore, the TPT deficiency in *ape2* plants and its direct consequences on carbon metabolism within the chloroplast do not themselves provide signals sufficient to trigger starch turnover. A similar argument can be made for other aspects of metabolism outside the chloroplast. In particular, although reduced Suc levels provide signals repressing AGPase activity and starch synthesis in Arabidopsis leaves (Hendriks et al., 2003) and promoting starch mobilization in potato tubers (Tiessen et al., 2002), this cannot on its own explain why starch turnover occurs specifically in HL-grown *ape2* plants since Suc synthesis is also affected in LL plants. The specific induction of starch degradation in the mutant under HL implies the involvement of one or more signals that arise only under these conditions.

An obvious possibility is that there is a link between starch turnover in HL *ape2* plants and the finding that photosynthesis is phosphate-limited. Analysis of photosynthesis in these plants has revealed several potential signals that might activate starch turnover and that are observed or implied specifically in HL *ape2* plants. These include metabolic signals from lowered phosphate levels and a reduced ATP to ADP ratio, and redox signals from plastoquinone, NADP, and thioredoxins. All these signals have been shown to have regulatory roles within the chloroplast (Wedel and Soll, 1998; Kim et al., 1999; Rintamaki et al., 2000; Oswald et al., 2001; Kim and Mayfield, 2002). However, phosphate depletion is a key signal known to promote starch synthesis through the activation of AGPase (Sowokinos, 1981; Sowokinos and Preiss, 1982; Hendriks et al., 2003). Similarly, although the chloroplast ATP to ADP ratio may be reduced compared to HL-grown wild type, it is nevertheless probably greater than that for LL-grown plants, which show no starch turnover, since ATP/ADP is known to correlate with the rate of photosynthesis (Brooks et al., 1988). The strongest candidate signals are therefore redox changes in plastoquinone, NADP, and thioredoxins.

Light-dependent redox signals (probably including thioredoxins) have been shown to regulate AGPase in combination with Suc (Hendriks et al., 2003). However, redox signaling within the chloroplast is complex, with the response to one signal being modulated by others. For instance, during photosynthetic acclimation, a reduced plastoquinone pool can have opposite effects depending on whether the stroma is oxidized (in which case there is a reduction in the relative levels of PSII) or reduced (leading to increased PSII levels; Pfannschmidt et al., 1999; Walters et al., 2003). In much the same way, signals from reduced plastoquinone leading to phosphorylation of light-harvesting complexes are subject to attenuation by reduced thioredoxins (Rintamaki et al., 2000). Therefore, the precise signal generated depends on the relative redox states of different redox components. It is tempting to speculate that the redox changes brought about in HL *ape2* plants are such as to activate starch breakdown, perhaps in conjunction with signals resulting from low Suc levels. There is an attractive symmetry to a hypothesis in which Suc and redox signals combine to regulate in a reciprocal manner the synthesis and breakdown of starch.

The importance of starch as a store of carbohydrate, which is released overnight, is demonstrated by the poor growth of mutants deficient in its synthesis or degradation (Caspar et al., 1991; Schneider et al., 2002; Sun et al., 2002). However, although it is known that levels of other carbohydrates influence starch breakdown (Hill and ap Rees, 1995; Loreti et al., 2003) and that many of the genes encoding putative components of the starch degradative machinery are regulated in a circadian fashion (Harmer et al., 2000), the regulatory mechanisms determining the timing and extent of starch degradation are largely unknown. The turnover of starch in TPT-deficient plants specifically under HL conditions is likely to reflect the aberrant activation of one or more signals—starch breakdown in the light does not appear to be a normal feature of wild-type plants (Zeeman et al., 2002)—and provides a tightly controlled system within which to investigate the regulation of starch turnover. The finding that starch breakdown is triggered in *ape2* plants by a simple change in growth conditions, without any change in the expression of genes involved in starch metabolism, clearly indicates that it is regulated by components of metabolism rather than in response to external triggers. Further analysis of this system offers the prospect of identifying the signals involved and the ways in which they serve to regulate the release of stored carbohydrate.

MATERIALS AND METHODS

Plant Material and Growth Conditions

Arabidopsis L. (Heynh.) cv Wassilewskija (Ws-2, N1601) and the *ape2* mutant derived from it (Walters et al., 2003) were grown from seed in growth chambers with an 8-h photoperiod at a photon flux density of 100 μmol quanta m^{-2} s^{-1} (LL) or 400 μmol quanta m^{-2} s^{-1} (HL) as described previously (Walters et al., 1999).

RNA and Protein Analyses

Unshaded mature leaves were excised from intact plants under growth conditions 2 h into the photoperiod and were immediately frozen in liquid nitrogen and stored at −80°C until use. For RT-PCR, total RNA was extracted using the RNeasy protocol (Qiagen, Venlo, The Netherlands), and 1 μg was annealed to 10 μM oligo(dT) in 15 μL of total volume (10 min at 70°C, 5 min on ice). cDNA was then synthesized using MMLV-RT (Promega, Madison WI) in the presence of 40 units RNasin (Promega). RT-PCR (using cDNA usually corresponding to 120 pg of total RNA per 50-μL reaction) was carried out with cycle parameters empirically determined for each primer pair to give a reproducibly linear relationship between message abundance and product yield over a 10-fold range. Primer pairs spanned one or more introns, allowing confirmation that only cDNA was amplified: *TPT*, 5′-TGATACCAGTCGCAGTCTGT-3′, 5′-CTCTCCAAGGTATTGGTAGC-3′; *GPT*,

5′-TGATGATGCTT(A/G)TCTCTTGG-3′, 5′-TAGTAGTTCAT(C/T)CCGCTCAC-3′; *PPT*, 5′-CAACAT(C/T)T(A/T)CAA(C/T)AAACAGG-3′, 5′-TC(G/T)CCAATATCAT(G/A)TACGA-3′; *Act4*, 5′-GTCATCTTCTCACGGTTAGC-3′, 5′-GGACGGTGAAGACATTCAAC-3′. Microarray experiments using the Arabidopsis full-genome GeneChip (ATH1-121501; Affymetrix, Santa Clara, CA) were carried out by the Nottingham Arabidopsis Stock Centre Transcriptomics Service (Craigon et al., 2004); each experiment (three for each set of plants) used independent preparations of 20 μg of total RNA extracted from leaves harvested 2 h into the photoperiod (our unpublished data).

Chloroplast envelope membranes were isolated essentially according to Barnes et al. (1994). Freshly harvested leaves from 8 plants were ground in an ice-cold mortar and pestle with 10 mL of extraction buffer (10 mM Tricine-KOH, 2 mM Na_2EDTA, pH 7.6). After centrifugation to remove debris and starch (10,000*g*, 30 s) and removal of an aliquot for chlorophyll determination, the supernatant was applied to a Suc step gradient (10 mL of 0.6 M Suc and 10 mL of 1.0 M Suc, both in extraction buffer) and centrifuged (60,000*g*, 2 h). The band at the 0.6 M/1.0 M Suc interface was removed and washed by addition of 10 mL of extraction buffer. Finally, envelope membranes were sedimented by centrifugation (100,000*g*, 1 h) and resuspended in 100 μL of extraction buffer. One to 5 μL of envelope preparations were separated by SDS-PAGE (Laemmli, 1970), and proteins were visualized by silver staining (Silver Stain Plus; Bio-Rad, Hercules CA).

Carbohydrate Assays

Leaf discs (1 cm^2, approximately 20 mg fresh weight) were cut from LL-grown plants at 2-h intervals throughout an 8-h photoperiod and immediately frozen in liquid N_2. Subsequently, they were extracted successively for 10 min in 1 mL of 80% (v/v) ethanol, 1 mL of 50% (v/v) ethanol, 1 mL of 20% (v/v) ethanol, 1 mL of water, and finally 1 mL of 80% (v/v) ethanol. The extracts were combined, dried down under vacuum, and redissolved in 0.5 mL of water. Glc and Fru in the ethanol-soluble fraction were measured enzymically (Morrell and ap Rees, 1986). Suc was measured after hydrolysis to Glc and Fru by incubation in 75 mM citric acid at 90°C for 2 h and subsequent addition of Tris-HCl (pH 7.5) to a final concentration of 400 mM.

For assays of starch, the ethanol-insoluble material was homogenized in 200 μL of water and autoclaved at 121°C (114 kPa) for 3 h. The suspension was then adjusted to 25 mM Na-citrate (pH 4.8) and incubated with 3 units porcine pancreas α-amylase and 1 unit amyloglucosidase (special quality for starch determination) for 16 h at 37°C. The digested material was centrifuged at 13,000*g* for 5 min, and the Glc content of the resulting supernatant was determined as above. All auxiliary enzymes were from Roche Diagnostics (Lewes, East Sussex, UK).

Photosynthesis in $^{14}CO_2$

Five to 6 weeks after germination, 9 or 12 plants were placed in a sealed glass chamber (36.5 × 26.5 × 24.5 cm, total volume 23.7 dm^3) and exposed to $^{14}CO_2$ 1 h into the photoperiod. The $^{14}CO_2$ was released inside the chamber by injecting 1 mL of propionic acid into 50 μL or 100 μL of 1 M $NaH^{14}CO_3$ (specific activity 37 GBq mol^{-1}) contained in a vial suspended inside the chamber. Two small electric fans were used to circulate air within the chamber. After 15 min the chamber was flushed with air for 5 min (flow rate 9 dm^3 min^{-1}). Plants were then removed from the chamber or (in pulse-chase experiments) incubated in the opened container for a further 2 or 4 h. Throughout the incubation plants were exposed to the irradiance under which they were grown and the temperature remained at 20°C. After harvesting, the aerial portion of each plant was immediately placed in a tube containing 20 mL of ethanol at 0°C, rapidly frozen in liquid nitrogen, and then stored at −80°C. For pulse-chase experiments, each plant was photographed at the start of the experiment to allow determination of rosette area; this was used to compare plants since it reflects the relative rate of light capture and therefore of overall photosynthesis.

Extraction of Leaf Material Using Aqueous Ethanol

Frozen aerial tissue from each plant was extracted by boiling for 10 min successively in 20 mL of 100% (v/v) ethanol, 20 mL of 20% (v/v) ethanol, 20 mL of water, and finally twice in 20 mL of 100% (v/v) ethanol. The supernatants were combined and dried by rotary evaporation under vacuum. The ethanol-soluble components were redissolved in 10 mL of 20% (v/v) aqueous ethanol.

Fractionation of ^{14}C-Labeled Extracts

The soluble fraction obtained following ethanol extraction was separated into acidic, basic, and neutral components by ion-exchange chromatography using Dowex 1X8-200 and Dowex 50WX8-200 (Sigma-Aldrich, Poole, Dorset, UK) as described previously (Runquist and Kruger, 1999). The neutral fraction was evaporated to dryness, resuspended in 50% (v/v) ethanol, and further fractionated by thin-layer chromatography on cellulose sheets (20 × 20 cm; Merck, Poole, Dorset, UK) in a solvent of formic acid:ethyl methyl ketone: tertiary butanol:water (30:60:80:30, by volume). Labeling of Suc was confirmed on the basis of its breakdown to Glc and Fru after digestion with 10% formic acid (4 h, 65°C). No appreciable labeling of high M_r ethanol-soluble glucans was observed.

The ethanol-insoluble fraction was homogenized with water in a final volume of 15 mL and autoclaved at 121°C for 3 h. A 1-mL aliquot of the autoclaved insoluble fraction was digested sequentially for 16 h at 37°C with 10 units amyloglucosidase (Roche) and 2 units amylase (Merck) in 50 mM Na-acetate (pH 5.8), and then with 10 units pronase (protease XIV *Streptomyces griseus*; Sigma-Aldrich) in 90 mM Tris-HCl (pH 7.8). Ion-exchange chromatography, as described above, was used to separate neutral, basic, and acidic fractions corresponding to starch, protein, and cell wall components, respectively. The insoluble residue, consisting of additional cell wall material, was washed three times with 0.5 mL of water, resuspended in 0.25 mL of water, and then incubated with 0.25 mL of tissue solubilizer (Merck) at 60°C for 24 h. The amount of radioactivity in the initial insoluble fraction was determined by incubating triplicate 0.25-mL aliquots of the autoclaved homogenate with 0.25 mL of tissue solubilizer at 60°C for 24 h.

Photosynthesis and Chlorophyll Fluorescence Measurements

Measurements of O_2 evolution in saturating CO_2 from leaf discs were carried out using an LD2 leaf-disc electrode as described previously (Walters et al., 1999). Measurements from attached leaves of CO_2 assimilation in air or with varying C_i were carried out using a Ciras-2 infrared gas analyzer (PP Systems, Hitchin, UK) with parallel analysis of chlorophyll fluorescence using a PAM100 fluorometer (H. Walz, Effeltrich, Germany) as described previously (Walters et al., 1999). Additional parallel measurement of PSI absorbance changes was performed using a second PAM100 fluorometer fitted with an ED-P700DW dual-wavelength emitter-detector unit. The redox states of P700 and of the PSI acceptor side were determined essentially according to Klughammer and Schrieber (1994). In situ chlorophyll fluorescence measurements under growth conditions were carried out using a PAM2000 fluorometer; the dark F_o' fluorescence level was measured immediately after growth lights were switched off.

Determination of Xanthophyll Composition

Unshaded mature leaves were excised from intact plants under growth conditions and immediately frozen in liquid nitrogen and stored at −80°C until use. Pigments were extracted in ethanol/diethyl ether, dried under N_2, redissolved in acetone, and analyzed by reverse-phase HPLC as described by Ruban et al. (1994) with the modifications described by Andersson et al. (2001).

Determination of NADP-MDH Activity

Unshaded mature leaves were excised from intact plants under growth conditions and immediately frozen in liquid nitrogen and stored at −80°C until use. Individual frozen leaves (about 100 mg fresh weight) were ground to a fine powder using a microhomogenizer driven by an electric drill (Hearse, 1984) and extracted in 0.5 mL of 50 mM sodium acetate (pH 6.0) that had been previously degassed and bubbled with nitrogen, supplemented with 1 mg mL^{-1} bovine serum albumin, 0.04 mM 4-(2-aminoethyl)benzenesulfonyl fluoride hydrochloride, 4 mM dithiothreitol, and 0.1% (v/v) Triton X-100. The suspension was mixed until homogeneous, centrifuged at 13,500*g* for 5 min, and the resulting supernatant used for determination of enzyme activity. The activity of NADP-MDH was measured spectrophotometrically as the oxaloacetate-dependent rate of cofactor oxidation as described by Scheibe and Stitt (1988). Apparent NADP-dependent MDH activity was measured in an assay containing 100 mM Tris-HCl (pH 8.0), 1 mM EDTA, 1 mM dithiothreitol,

0.2 mM NADPH, and 2 mM oxaloacetate. Total NADP-dependent MDH capacity was determined following complete reductive activation by incubating an aliquot of the extract with half a volume of 0.5 M dithiothreitol (pH 8.0) and half a volume of 1 M Tris-HCl (pH 9.0) at room temperature for 40 min. The activity of NAD-MDH was determined in diluted samples of extract in an assay containing 100 mM Tris-HCl (pH 8.0), 1 mM EDTA, 10 mM $MgCl_2$, 0.2 mM NADH, and 2 mM oxaloacetate. All assays were conducted in a final volume of 0.25 mL in a microtiter plate at 30°C. The fractional activation state of stromal NADP-MDH was calculated assuming that the contribution of NAD-MDH to the NADP-dependent MDH activity was 0.2% of the total NAD-dependent activity (Scheibe and Stitt, 1988).

ACKNOWLEDGMENTS

We thank Mrs. P. Scholes for excellent technical assistance.

Received February 6, 2004; returned for revision March 11, 2004; accepted March 11, 2004.

LITERATURE CITED

Andersson J, Walters RG, Horton P, Jansson S (2001) Antisense inhibition of the photosynthetic antenna proteins CP29 and CP26: implications for the mechanism of protective energy dissipation. Plant Cell **13:** 1193–1204

Ashton AR, Trevanion SJ, Carr PD, Verger D, Ollis DL (2000) Structural basis for the light regulation of chloroplast NADP malate dehydrogenase. Physiol Plant **110:** 314–321

Bailey S, Horton P, Walters RG (2004) Acclimation of *Arabidopsis thaliana* to the light environment: the relationship between photosynthetic function and chloroplast composition. Planta **218:** 793–802

Barnes SA, Knight JS, Gray JC (1994) Alteration of the amount of the chloroplast phosphate translocator in transgenic tobacco affects the distribution of assimilate between starch and sugar. Plant Physiol **106:** 1123–1129

Brooks A, Portis AR, Sharkey TD (1988) Effects of irradiance and methyl viologen treatment on ATP, ADP, and activation of ribulose bisphosphate carboxylase in spinach leaves. Plant Physiol **88:** 850–853

Caspar T, Lin TP, Kakefuda G, Benbow L, Preiss J, Somerville C (1991) Mutants of *Arabidopsis* with altered regulation of starch degradation. Plant Physiol **95:** 1181–1188

Craigon DJ, James N, Okyere J, Higgins J, Jotham J, May S (2004) NASCArrays: A repository for microarray data generated by NASC's transcriptomics service. Nucleic Acids Res **32:** D575–D577

Edwards G, Walker DA (1983) C3, C4, Mechanisms, and Cellular and Environmental Regulation of Photosynthesis. Blackwell Scientific, Oxford, UK

Eskling M, Arvidsson PO, Akerlund HE (1997) The xanthophyll cycle, its regulation and components. Physiol Plant **100:** 806–816

Harmer SL, Hogenesch LB, Straume M, Chang HS, Han B, Zhu T, Wang X, Kreps JA, Kay SA (2000) Orchestrated transcription of key pathways in Arabidopsis by the circadian clock. Science **290:** 2110–2113

Hattenbach A, Muller-Rober B, Nast G, Heineke D (1997) Antisense repression of both ADP-glucose pyrophosphorylase and triose phosphate translocator modifies carbohydrate partitioning in potato leaves. Plant Physiol **115:** 471–475

Häusler RE, Schlieben NH, Flügge UI (2000b) Control of carbon partitioning and photosynthesis by the triose phosphate/phosphate translocator in transgenic tobacco plants (*Nicotiana tabacum*). II. Assessment of control coefficients of the triose phosphate/phosphate translocator. Planta **210:** 383–390

Häusler RE, Schlieben NH, Nicolay P, Fischer K, Fischer KL, Flügge UI (2000a) Control of carbon partitioning and photosynthesis by the triose phosphate/phosphate translocator in transgenic tobacco plants (*Nicotiana tabacum* L.). I. Comparative physiological analysis of tobacco plants with antisense repression and overexpression of the triose phosphate/phosphate translocator. Planta **210:** 371–382

Häusler RE, Schlieben NH, Schulz B, Flügge UI (1998) Compensation of decreased triose phosphate phosphate translocator activity by accelerated starch turnover and glucose transport in transgenic tobacco. Planta **204:** 366–376

Hearse DJ (1984) Microbiopsy metabolite and paired flow-analysis – a new rapid procedure for homogenization, extraction and analysis of high-energy phosphates and other intermediates without any errors from tissue loss. Cardiovasc Res **18:** 384–390

Heineke D, Kruse A, Flügge UI, Frommer WB, Riesmeier JW, Willmitzer L, Heldt HW (1994) Effect of antisense repression of the chloroplast triose-phosphate translocator on photosynthetic metabolism in transgenic potato plants. Planta **193:** 174–180

Hendriks JHM, Kolbe A, Gibon Y, Stitt M, Geigenberger P (2003) ADP-glucose pyrophosphorylase is activated by posttranslational redox-modification in response to light and to sugars in leaves of *Arabidopsis* and other plant species. Plant Physiol **133:** 838–849

Hill SA, ap Rees T (1995) The effect of glucose on the control of carbohydrate-metabolism in ripening bananas. Planta **196:** 335–343

Kim M, Christopher DA, Mullet JE (1999) ADP-dependent phosphorylation regulates association of a DNA-binding complex with the barley chloroplast *psbD* blue-light-responsive promoter. Plant Physiol **119:** 663–670

Kim J, Mayfield SP (2002) The active site of the thioredoxin-like domain of chloroplast protein disulfide isomerase, RB60, catalyzes the redox-regulated binding of chloroplast poly(A)-binding protein, RB47, to the 5′ untranslated region of *psbA* mRNA. Plant Cell Physiol **43:** 1238–1243

Klughammer C, Schrieber U (1994) An improved method, using saturating light-pulses, for the determination of photosystem I quantum yield via $P700^+$ absorbency changes at 830 nm. Planta **192:** 261–268

Kramer DM, Sacksteder CA, Cruz JA (1999) How acidic is the lumen? Photosynth Res **60:** 151–163

Krause GH, Weis E (1991) Chlorophyll fluorescence and photosynthesis – the basics. Annu Rev Plant Physiol Plant Mol Biol **42:** 313–349

Laemmli UK (1970) Cleavage of the structural proteins during the assembly of the head of bacteriophage T4. Nature **227:** 680–685

Loreti E, Yamaguchi J, Alpi A, Perata P (2003) Sugar modulation of alpha-amylase genes under anoxia. Ann Bot **91:** 143–148

Morrell S, ap Rees T (1986) Control of the hexose content of potato-tubers. Phytochemistry **25:** 1073–1076

Nielsen TH, Baunsgaard L, Blennow A (2002) Intermediary glucan structures formed during starch granule biosynthesis are enriched in short side chains, a dynamic pulse labeling approach. J Biol Chem **277:** 20249–20255

Niittylä T, Messerli G, Trevisan M, Chen J, Smith AM, Zeeman SC (2004) A previously unknown maltose transporter essential for starch degradation in leaves. Science **203:** 87–89

Oswald O, Martin T, Dominy PJ, Graham IA (2001) Plastid redox state and sugars: interactive regulators of nuclear-encoded photosynthetic gene expression. Proc Natl Acad Sci USA **98:** 2047–2052

Ott T, Clarke J, Birks K, Johnson G (1999) Regulation of the photosynthetic electron transport chain. Planta **209:** 250–258

Pfannschmidt T, Nilsson A, Allen JF (1999) Photosynthetic control of chloroplast gene expression. Nature **397:** 625–628

Riesmeier JW, Flügge UI, Schulz B, Heineke D, Heldt HW, Willmitzer L, Frommer WB (1993) Antisense repression of the chloroplast triose phosphate translocator affects carbon partitioning in transgenic potato plants. Proc Natl Acad Sci USA **90:** 6160–6164

Rintamaki E, Martinsuo P, Pursiheimo S, Aro EM (2000) Cooperative regulation of light-harvesting complex II phosphorylation via the plastoquinol and ferredoxin-thioredoxin system in chloroplasts. Proc Natl Acad Sci USA **97:** 11644–11649

Ruban AV, Young AJ, Pascal AA, Horton P (1994) The effects of illumination on the xanthophyll composition of the photosystem II light-harvesting complexes of spinach thylakoid membranes. Plant Physiol **104:** 227–234

Runquist M, Kruger NJ (1999) Control of gluconeogenesis by isocitrate lyase in endosperm of germinating castor bean seedlings. Plant J **19:** 423–431

Scheibe R, Stitt M (1988) Comparison of NADP-malate dehydrogenase activation, Q_A reduction and O_2 evolution in spinach leaves. Plant Physiol Biochem **26:** 473–481

Schneider A, Häusler RE, Kolukisaoglu U, Kunze R, van der Graaff E, Schwacke R, Catoni E, Desimone M, Flügge UI (2002) An *Arabidopsis thaliana* knock-out mutant of the chloroplast triose phosphate/phosphate translocator is severely compromised only when starch synthesis, but not starch mobilisation is abolished. Plant J **32:** 685–699

Sharkey TD, Savitch LV, Vanderveer PJ, Micallef BJ (1992) Carbon partitioning in a *Flaveria linearis* mutant with reduced cytosolic fructose bisphosphatase. Plant Physiol **100:** 210–215

Sharkey TD, Stitt M, Heineke D, Gerhardt R, Raschke K, Heldt HW (1986) Limitation of photosynthesis by carbon metabolism. II. O_2 insensitive CO_2 uptake results from limitation of triose phosphate utilization. Plant Physiol **81:** 1123–1129

Sowokinos JR (1981) Pyrophosphorylases in *Solanum tuberosum*. 2. Catalytic properties and regulation of ADP-glucose and UDP-glucose pyrophosphorylase activities in potatoes. Plant Physiol **68:** 924–929

Sowokinos JR, Preiss J (1982) Pyrophosphorylases in *Solanum tuberosum*. 3. Purification, physical, and catalytic properties of ADP-glucose pyrophosphorylase in potatoes. Plant Physiol **69:** 1459–1466

Strand A, Zrenner R, Trevanion S, Stitt M, Gustafsson P, Gardestrom P (2000) Decreased expression of two key enzymes in the sucrose biosynthesis pathway, cytosolic fructose-1,6-bisphosphatase and sucrose phosphate synthase, has remarkably different consequences for photosynthetic carbon metabolism in transgenic Arabidopsis thaliana. Plant J **23:** 759–770

Sun JD, Gibson KM, Kiirats O, Okita TW, Edwards GE (2002) Interactions of nitrate and CO2 enrichment on growth, carbohydrates, and Rubisco in *Arabidopsis* starch mutants. Significance of starch and hexose. Plant Physiol **130:** 1573–1583

Tiessen A, Hendriks JHM, Stitt M, Branscheid A, Gibon Y, Farre EM, Geigenberger P (2002) Starch synthesis in potato tubers is regulated by post-translational redox modification of ADP-glucose pyrophosphorylase: a novel regulatory mechanism linking starch synthesis to the sucrose supply. Plant Cell **14:** 2191–2213

Tiessen A, Prescha K, Branscheid A, Palacios N, McKibbin R, Halford NG, Geigenberger P (2003) Evidence that SNF1-related kinase and hexokinase are involved in separate sugar-signalling pathways modulating post-translational redox activation of ADP-glucose pyrophosphorylase in potato tubers. Plant J **35:** 490–500

Walker DA (1992) Concerning oscillations. Photosynth Res **34:** 387–395

Walters RG, Rogers JJM, Shephard F, Horton P (1999) Acclimation of *Arabidopsis thaliana* to the light environment: the role of photoreceptors. Planta **209:** 517–527

Walters RG, Shephard F, Rogers JJM, Rolfe SA, Horton P (2003) Identification of mutants of *Arabidopsis* defective in acclimation of photosynthesis to the light environment. Plant Physiol **131:** 472–481

Wedel N, Soll J (1998) Evolutionary conserved light regulation of Calvin cycle activity by NADPH-mediated reversible phosphoribulokinase/CP12/glyceraldehyde-3-phosphate dehydrogenase complex dissociation. Proc Natl Acad Sci USA **95:** 9699–9704

Weise SE, Weber APM, Sharkey TD (2004) Maltose is the major form of carbon exported from the chloroplast at night. Planta **218:** 474–482

Zeeman SC, Tiessen A, Pilling E, Kato KL, Donald AM, Smith AM (2002) Starch synthesis in *Arabidopsis*. Granule synthesis, composition, and structure. Plant Physiol **129:** 516–529

Zrenner R, Krause KP, Apel P, Sonnewald U (1996) Reduction of the cytosolic fructose-1,6-bisphosphatase in transgenic potato plants limits photosynthetic sucrose biosynthesis with no impact on plant growth and tuber yield. Plant J **9:** 671–681